Military Technical College
Kobry El-Kobbah,
Cairo, Egypt

14th International Conference on Applied Mechanics and Mechanical Engineering.

Effect of soil on the vibration and stability of buried composite material pipes conveying fluid

By

R. M. Gadelrab, E. Rabeih and A.A. Atwa

Abstract:

This work is concerned with the investigation of the free vibration and stability behavior of the buried composite material pipes. Soil is modeled mathematically as a one and two parameters foundation, (Winkler and Pasternak respectively). Composite material is treated as generally orthotropic material and the flow is a fully turbulent flow. A mathematical model based on Timoshenko beam theory is formulated. A finite element model has been implemented to investigate the problem. Mat lab package has been used to construct a program for vibration and stability analysis of the system. The obtained results have been compared with the published ones to verify the model. A comparison between buried composite material pipes and traditional ones is presented. The results show that the soil modeling, internal pressure and depth of the soil have an essential effect on the behavior of such pipes.

Keywords:

composite material pipes

1 Prof., Mechanical Design Department, Faculty of Engineering, Mataria, Helwan. Dean of Elsalam Higher Institute of Engineeing and Technology
2 Ass. Prof. Mechanical Design Department, Faculty of Engineering, Mataria, Helwan.
3 Lecturer, Canadian Higher Institute for engineering, CIC, Manufacture department.

Introduction:

Piping systems are widely used in modern industry in fluid and oil transportation. In some applications, the fluid in the piping system has high flow velocities like the nuclear reactors and in steam generator. These high flow velocities can cause a damage of the system due to instability of the system at certain flow velocities [1]. Buried pipes can sustain to this instability. It is well known that, the pipes is dynamically stable at low flow velocity and according to the configuration and boundary conditions the system lose its stability in buckling mode at certain velocity, like beam subjected to compressive load. When the system is a conservative, it loses its stability in a coupled mode flutter in higher modes [2]. While the non-conservative system loses its stability in flutter mode. The cause of this instability types is mainly due to follower force which the fluid is subjected in the course of lateral motion of the pipe. Material properties have a reasonable effect on the critical flow velocity, the velocity at which the system loses its stability. On the other hand, composite material parameters like fiber orientation angles and stacking order affect the dynamic behavior of such systems. The same authors, [3], introduced a work discuss the effect of composite materials parameters on the critical flow velocity of such system. A comparison between the traditional material and composite one was introduced.

As known, the composite material dynamic governing differential equation of motion is sixth order differential equation rather than the traditional one which is a forth order. Therefore, the traditional material model cannot be used for composite one. Also the shear effect in composite material has a major effect due to the nature of material [4], therefore, thick beam theory is essential to use in the case of dealing with composite material. Composite materials have a competitive chemical and stiffness to weight ratio comparing to traditional material ones. Therefore, it is preferable to use it in some applications.

For buried pipes, soil is a complicated material and there are still great uncertainties on how to deal analytically with partially saturated soils [5]. In this paper, soil is modeled as one (Winkler) and Two (Pasternak) parameters foundation to investigate the effect of the soil on the stability and behavior of such problem. Pasternak model is more convenient for the soil due to the nature of soil which is the shear interaction between adjacent soil elements [6].

The pipeline is generally simplified as a beam, while pipe–soil interaction is represented by soil springs in the axial (or longitudinal), transverse horizontal, and transverse vertical directions using a Winkler or Pasternak type model. The properties of soil springs in three orthogonal directions are independent. In other words, the deformation of soil in one direction has no effect on pipe–soil interactions in other directions. The initial stiffness K of the force–displacement curve depends on the elastic modulus of the soil E, the diameter of the pipe, and the buried depth ratio H/D. Damping of soil is a major parameter in the behavior of such system [7]. The damping of soil is modeled as a proportional damping [8].

In this paper, the vibration and stability behavior of the composite material buried pipes conveying fluids is concerned. The finite element technique is suggested to model and investigate this problem. The stability of pipes is governed by the natural frequencies, which are greatly affected by flow velocities, soil parameters and pipe depth. The soil is modeled as soft and medium clay. A comparison between two foundation types is presented and a comparison between traditional and composite materials is discussed. The effect of soil damping is introduced.

Mathematical Model:

The composite materials are anisotropic material where its properties are direction dependent. In this material, the coupling between bending and twisting should be considered. The finite element technique has been used to obtain the equation of motion of composite material pipes. The model is based on Timoshenko beam theory. Figure (1) shows a pipe element conveying steady fluid with velocity (v). In the element shown, three degrees of freedom at each node has been considered namely; lateral displacement (y), cross section rotation (ψ) and cross section twisting (ϕ). Note that; 1, 2, 3 are the principal axes of the element and X, Y, Z, are the geometric coordinates.
The strain energy of the pipe element (see the list of symbols in appendix) is [2,6];

$$U = \int_0^L \left(\begin{array}{l} \frac{1}{2} M \frac{\partial \psi}{\partial x} + \frac{1}{2} T \frac{\partial \phi}{\partial x} + \frac{1}{2}\left(\frac{\partial y}{\partial x} - \psi\right) Q + \frac{1}{2} P \left(\frac{dy}{dx}\right)^2 + \frac{1}{2} K_w y^2 + \\ \frac{1}{2} K_P \left(\frac{dy}{dx}\right)^2 + \frac{1}{2} P_r A (1 - 2\upsilon) \left(\frac{dy}{dx}\right)^2 \end{array} \right) dx \qquad (1)$$

Where

$\frac{1}{2} M \frac{\partial \psi}{\partial z}$ and $\frac{1}{2} T \frac{\partial \phi}{\partial z}$ are the strain energies due to bending (M) and twisting (T) moments respectively [11].

$\frac{1}{2}\left(\frac{\partial y}{\partial z} - \psi\right) Q$ is the strain energy due to the shear force.

$M = \left(\frac{E_{zz} I_x}{\eta}\right)\left(\frac{\partial \psi}{\partial z}\right) + \left(\frac{C_t E_{zz} I_x}{\eta C_{mt}}\right)\left(\frac{\partial \phi}{\partial z}\right), \qquad T = \left(\frac{C_t}{\eta}\right)\left(\frac{\partial \phi}{\delta z}\right) + \left(\frac{C_t E_{zz} I_x}{\eta C_{mt}}\right)\left(\frac{\partial \psi}{\partial z}\right)$

and $Q = kAG_{xy}\left(\frac{d\mu}{dz} - \psi\right)$ is the shear force

The generalized torsional rigidity C_t and mutual rigidity, C_{mt}, are expressed as[9];

$C_t = pi \times (b^4 - a^4)/64 \times \sum_1^n Q_{23}$ and $C_{mt} = 2I_x / S_{36}$ where

$$S_{36} = 2\left(\frac{\sin^2\theta}{E_{11}} - \frac{\cos^2\theta}{E_{33}}\right)\sin\theta\cos\theta + \left(\frac{1}{G_{13}} - \frac{2\mu_{31}}{E_{33}}\right)\left(\cos^3\theta\right)\sin\theta$$

Q_{23} is the stiffness matrix element.

θ is the angle between the geometric coordinate system and principle axes.

The shear coefficient for orthotropic beam is [10]; $k = \frac{E_x}{2E_x - G_{xy}\mu_{xy}}$

P is the compressive force and P_r is the internal pressure

K_w Winkler foundation value [7]= $K_w = \frac{\beta_k E D}{(1-\nu^2)}\sqrt{\frac{H}{D}}$

K_p Pasternak foundation value

The kinetic energy of the pipe element is;

$$KE = \int_0^L \frac{1}{2}\rho_p A_p\left(\frac{\partial y}{\partial t}\right)^2 + \frac{1}{2}\rho_p J_{xy}\left(\frac{\partial \phi}{\partial t}\right)^2 + \frac{1}{2}\rho_p I_p\left(\frac{\partial \psi}{\partial t}\right)^2 + \frac{1}{2}\rho_f A_f\left(\frac{\partial y}{\partial t}\right)^2 + \frac{1}{2}\rho_f I_f\left(\frac{\partial \psi}{\partial t}\right)^2 + \frac{1}{2}\rho_f A_f\left(V^2 + \left(\frac{dy}{dt} + V\frac{dy}{dx}\right)^2\right)\mathrm{dz} \quad (2)$$

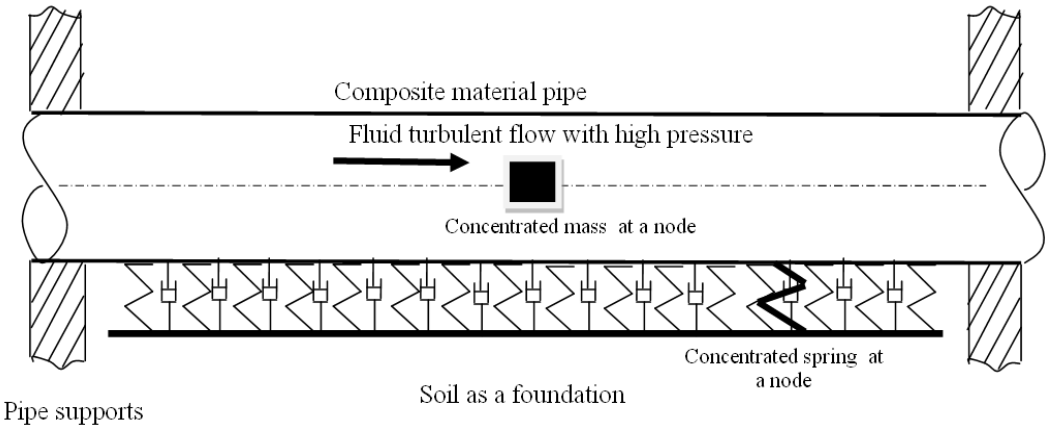

Figure (1) Model scematic drawing

Where

$\frac{1}{2}\rho_p A_p\left(\frac{\partial y}{\partial t}\right)^2$ and $\frac{1}{2}\rho_f A_f\left(\frac{\partial y}{\partial t}\right)^2$ are the kinetic energies due to the translation of pipe and fluid masses respectively.

$\frac{1}{2}\rho J_{xy}\left(\frac{\partial \phi}{\partial t}\right)^2$ and $\frac{1}{2}\rho_p I_p\left(\frac{\partial \psi}{\partial t}\right)^2$ are the kinetic energies due to twisting and bending rotary inertia of the pipe cross section respectively.

$\frac{1}{2}\rho_f I_{xf}\left(\frac{\partial \psi}{\partial t}\right)^2$ and $\frac{1}{2}\rho_f A_f\left(V^2 + \left(\frac{dy}{dt} + V\frac{dy}{dx}\right)^2\right)$ are the kinetic energies due to the fluid rotary inertia and the fluid flow velocity respectively.

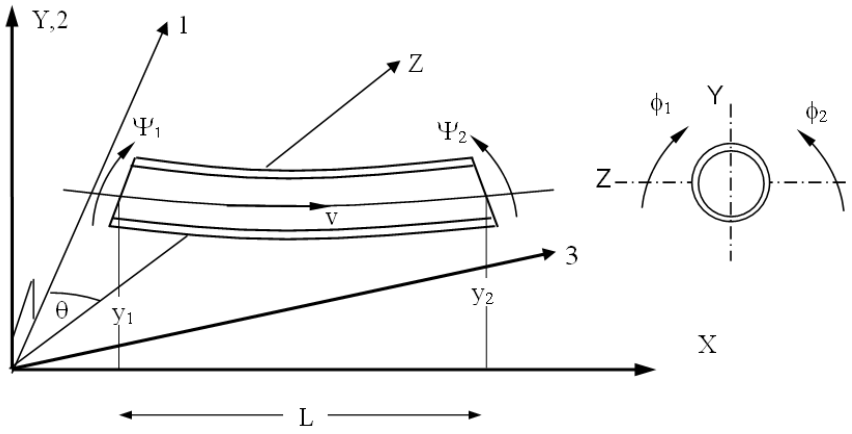

Figure (2) Pipe element

The modified stiffness matrix for composite material is expressed as[12]

$$[K]_1 = \int_0^1 [B]^T [K][B] d\xi$$

where

$$[K] = \begin{bmatrix} \frac{\eta}{s^2\lambda} & 0 & 0 & -\frac{\eta}{s^2\lambda} \\ 0 & \frac{1}{\lambda} & \frac{\alpha}{\lambda} & 0 \\ 0 & \frac{\alpha}{\lambda} & 1 & 0 \\ -\frac{\eta}{s^2\lambda} & 0 & 0 & \frac{\eta}{s^2\lambda} \end{bmatrix}$$

The stiffness matrix K for a certain node is presented the three degrees of freedom, ψ , Φ, and Φ' which implement a more accurate results for such type of materials.

And the matrix B whose its elements b_{ii} in the appendix A

$$[B]_1 = \begin{bmatrix} b_{11} & b_{12} & 0 & b_{14} & b_{15} & 0 \\ b_{21} & b_{22} & 0 & b_{14} & b_{15} & 0 \\ b_{31} & b_{32} & b_{33} & b_{34} & b_{35} & b_{36} \\ b_{41} & b_{42} & 0 & b_{44} & b_{45} & 0 \end{bmatrix}$$

The kinetic energy of the composite pipe element is;

$$KE = \int_0^L \{\frac{1}{2}\rho_p A_p \left(\frac{\partial y}{\partial t}\right)^2 + \frac{1}{2}\rho_p J_{xy}\left(\frac{\partial \phi}{\partial t}\right)^2 + \frac{1}{2}\rho_p I_p \left(\frac{\partial \psi}{\partial t}\right)^2 \} \mathrm{dz}$$

Where

The nodal displacement vector of the pipe element is; $\{q\} = \{y_1 \quad \psi_1 \quad \phi_1 \quad y_2 \quad \psi_2 \quad \phi_2\}^T$

For modified mass matrix for composite material $M_1 = \int_0^1 [A]^T [M][A] d\xi$ where[12]

$$[M] = \begin{bmatrix} 1 & 0 & 0 \\ 0 & r^2 & 0 \\ 0 & 0 & q^2 \end{bmatrix}$$

Where M is the mass matrix for uncoupled bending-torsion modes.

and $[A] = \begin{bmatrix} a_{11} & a_{12} & 0 & a_{14} & a_{15} & 0 \\ a_{21} & a_{22} & 0 & a_{24} & a_{25} & 0 \\ a_{31} & a_{32} & a_{33} & a_{34} & a_{35} & a_{36} \end{bmatrix}$ is the shape function matrix whose elements a_{ij} , are listed in the appendix (B) in dimensionless form.

Applying Lagrange's equation yields the equations of motion as; $[M]\{\ddot{q}\} + [C]\{\dot{q}\} + [K]\{q\} = \{0\}$

Where [M] and [K] are 6x6 mass and stiffness matrices of the composite pipe respectively and [C] is the soil damping matrix and gyroscopic matrices. The gyroscopic matrix presented the gyroscopic damping due to Ceriollous force. The damping of soil can be introduced as

$$C = \eta M + \delta K$$

Where $2\omega_n\zeta_n = \eta + \delta\omega_n^2$

The viscous damping matrix is dependent on stiffness, mass and the natural modes of the soil column. The natural modes and the soil stiffness are derived from the shear wave velocity profile of the soil column.

Solution Technique: An efficient computer program has been implemented using MATLAB to formulate and solve the governed equations of motion. The program is designed in an interactive form allowing the user to specify the required model. The parameter that control the problem like fiber volume fraction, fiber orientation angle, pipe dimensions, pipe depth, flow velocity, soil foundation modeling, soil type, condition of flow, damping of soil …etc are user entered data.

Verification of the Model: In this section, a comparison between published results and ones of the present model for most of famous configuration of beams and piping systems made of traditional and materials supported on foundation is introduced to verify the current model. Table (1) shows the effect of the foundation stiffness on the critical flow velocity of pipe made of traditional material investigated in reference [14]. The results show that the foundation has stabilizing effect on the pipe. The value of the critical velocity increases with the foundation value increase. The foundation value affects the type of stability. As the value of foundation increased the type of stability of second mode become in flutter mode. The values of the critical flow velocity will be closed together as the foundation value increased. The difference between the current and the previous results increased as the foundation value increase due to the difference between the shear coefficients in both cases. But it does not affect the type of stability of foundation values.

Table (1): Effect of foundation stiffness on the critical flow velocity of traditional material

Critical flow velocity	Foundation value (N/m)							
	K=0	K=1	K=10	K=100	K=1000	K=2000	K=10000	K=2*10000
First buckling critical velocity	3.114 (3.129)	3.129 (3.145)	3.273 (3.287)	4.458 (4.463)	7.874 (7.977)	9.349 (9.429)	13.632 (13.978)	15.773 (16.334)[14]
Mode	First mode	First mode	First mode	First mode	First mode	First mode	First mode	First mode
second buckling critical velocity	6.054 (6.195)	6.056 (6.194)	6.076 (6.212)	6.258 (6.393)	9.334 (9.744)	10.582 (12.511)	13.737 (17.064)	15.864 (17.515)
Mode	second mode	second mode	second mode	second mode	second mode	third mode	third mode	third mode
Flutter critical velocity	6.107 (6.27)	6.109 6.272)	6.129 (6.282)	6.339 (6.414)	9.396 (9.754)	10.347 (10.313)	13.645 (14.415)	15.842 (17.025)
Mode	third mode	third mode	third mode	third mode	third mode	second mode	second mode	second mode

The current model is applying to composite material beams supporting on Winkler foundation, at fiber orientation of angle=5^0. The results in the table (2) show the effect of the foundation stiffness on the beam natural frequencies. The calculated values of natural frequencies are compared with ones in reference [15].

Table (2): Effect of foundation stiffness on the natural frequency of composite material beam

Critical flow velocity	Foundation value (N/m)							
	K=0	K=1	K=10	K=100	K=1000	K=2000	K=10^4	K=2*10^4
First buckling critical velocity	3.114 (3.129)	3.129 (3.145)	3.273 (3.287)	4.458 (4.463)	7.874 (7.977)	9.349 (9.429)	13.632 (13.978)	15.773 (16.334)[15]
mode	First mode							
second buckling critical velocity	6.054 (6.195)	6.056 (6.194)	6.076 (6.212)	6.258 (6.393)	9.334 (9.744)	10.582 (12.51)	13.737 (17.064)	15.864 (17.515)
mode	second mode					third mode		
Flatter critical velocity	6.107 (6.27)	6.109 6.272)	6.129 (6.282)	6.339 (6.414)	9.396 (9.754)	10.347 (10.31)	13.645 (14.415)	15.842 (17.025)
mode	third mode					second mode		

Figure (3) shows the effect of the foundation stiffness on the nondimensional natural frequencies using the current model.

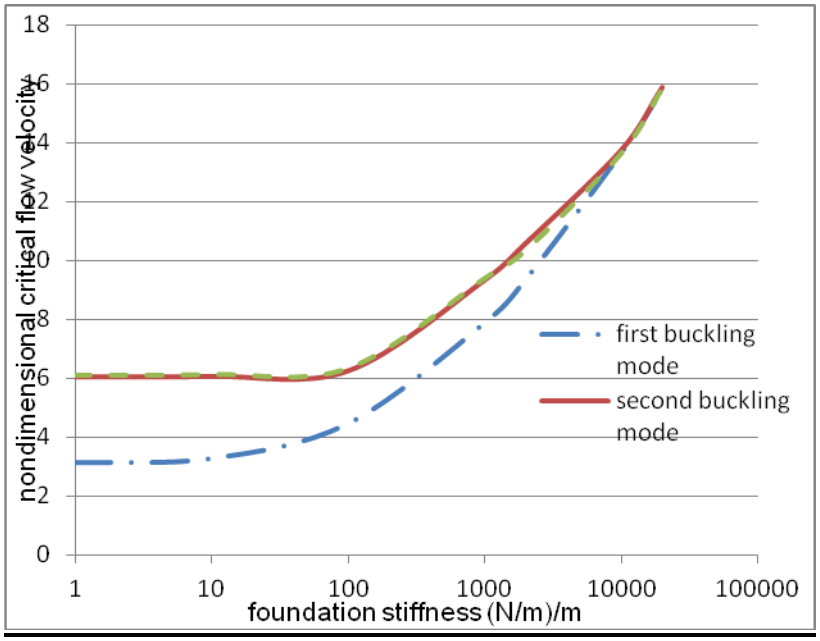

Figure(3): Effect of foundation on the critical flow velocity

From the above results, the current mathematical model and the implemented computer program are accurate and efficient tools and valid for further investigations of this area

Results and Discussion: A unidirectional typical composite material pipe made of glass fiber–epoxy conveying a steady fluid and buried in a soil has been considered here to investigate its dynamic and stability behavior. The behavior of a traditional material pipe (made of steel) is also investigated and compared with the composite material one. The composite material is generally orthotropic material and soil is handled as soft and medium clay with proportional damping. Effect of soil and pipe depth on the stability behavior of the pipe is introduced.
The properties of the considered composite material and steel, [11] are;

$E_{fiber} = 72.4e9\,\text{Pa}$ $\mu_{\text{fiber}} = 0.2$

$E_{matrix} = 4.1e9\,\text{Pa}$ $\mu_{\text{fiber}} = 0.35$

E_{steel}=200 x 10^9 Pa $\mu = 0.21$

The medium and soft clay properties are taken as shown in the tables (3) and (4) respectively

Table (3): Properties of medium clay [16]

Parameter	value
Modulus of Elasticity (E)	50 MPa
Friction angle	24^0
Cohesion C	15 (KPa)
Poisson ratio	0.25
Soil unit weight	17.7 (KN/m^3)

Table (4): Properties of soft clay

Parameter	value
Modulus of Elasticity (E)	10 MPa
Friction angle	26^0
Cohesion C	17 (KPa)
Poisson ratio	0.25
Soil unit weight	17.7 (KN/m^3)

Effect of pipe depth: Figure (4) indicates the difference in behavior of both types of soil (medium and soft clay) in its first mode. It is shown that the medium clay has a higher critical flow velocity than the soft one, the soil is assumed to be Winkler foundation.

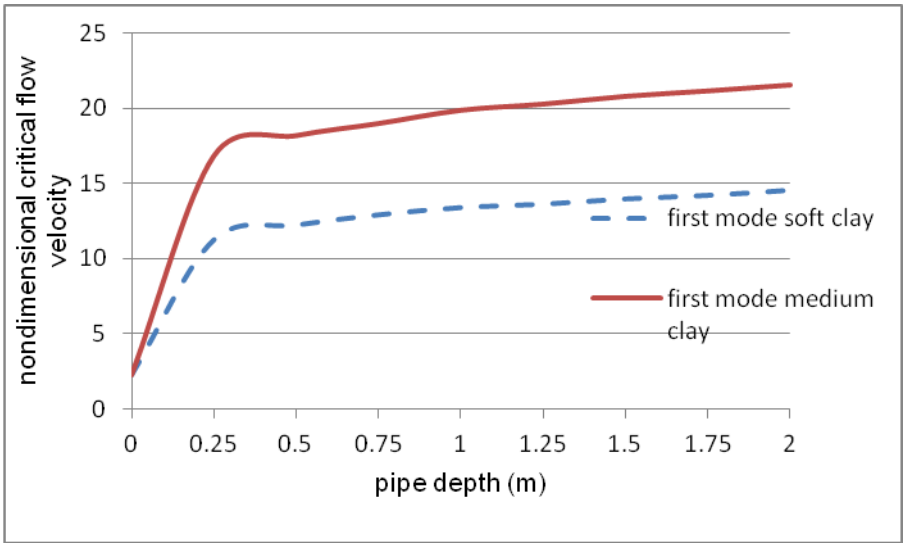

Figure (4): Comparison between soft and medium clay in the first mode.

Effect of soil model: Table (5) shows the difference between the effect of Winkler and Pasternak foundation on the critical flow velocity of the buried pipe at different soil depth. It is shown that the critical flow velocity increases when the soil is modeled as Pasternak foundation (for buried pipes). This is because the total strain energy increased due to added shear strain energy. The shear strain dependence mainly on the type of the soil and it is laboratory determined value. In this study it is assumed to be 0.1 from the value of Winkler foundation.

Table(5) non-dimensional critical flow velocity for Winkler and Pasternak foundation model at different soil depth (soft clay)

Depth (m)	First critical flow velocity		Second critical flow velocity	
	Winkler	Pasternak	Winkler	Pasternak
0 (unburied)	2.23	2.23	5.28	5.29
0.25	11.25	13.54	11.96	14.28
0.5	12.235	14.867	12.875	15.394
0.75	12.92	15.78	13.38	16.26
1	13.403	16.746	13.797	16.901
1.25	13.63	17.32	13.95	17.43
1.5	13.98	17.76	14.232	17.98
1.75	14.22	18.24	14.53	18.02
2	14.558	18.826	14.897	19.089

Figure (5) shows that the difference between critical flow velocities using the two models increases with the pipe depth increase. The value of critical velocity when soil is modeled as Pasternak foundation is higher than one for Winkler foundation.

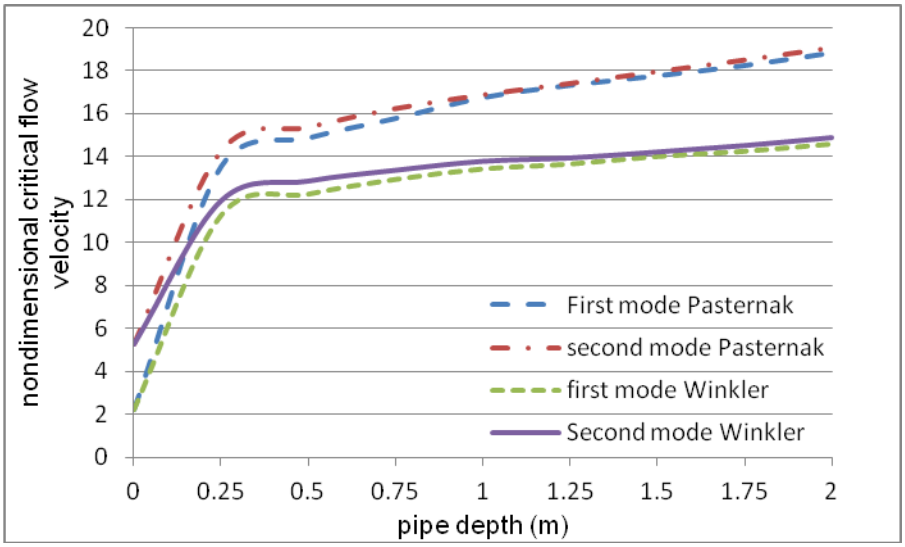

Figure (5) non-dimensional critical flow velocity using Winkler and Pasternak foundations with the pipe depth (soft clay)

The pipe depth is proportional to the foundation stiffness value of Winkler and Pasternak foundation.

Comparison between traditional and composite material pipe: Figure (6) shows a comparison between critical flow velocities of composite materials and steel pipes buried in medium clay in first and second modes.

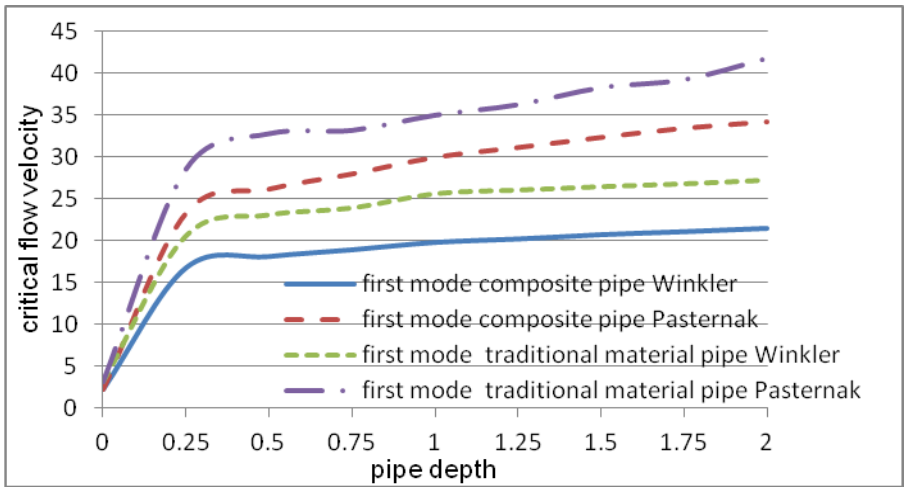

Figure (6) Comparison between composite material and traditional material pipe in it first mode (buckling mode) buried in medium clay.

This figure shows that, the non-dimensional critical flow velocity of buried composite pipe is lower than the steel one on both Winkler and Pasternak foundation models. Comparing figure 5 and 6, it is shown that pipes on medium clay has a higher critical flow velocity than one on the soft clay due to high elastic modulus of medium clay than soft clay. It is also noted that the difference between the two values are increased with the depth increase due to the increase of shear effect.

Effect of soil damping and gyroscopic action on the critical flow velocity and stability type: Soil damping can be modeled as a proportional damping in the form $\eta M + \delta K$. As the soil is modeled as Pasternak foundation, the value of η and δ depend mainly on the damping factor ξ and the soil natural frequency which can be determined in laboratory for different types of soil. The critical flow velocity of the damped system is shown below at different values of foundation stiffness. The gyroscopic effect is also included and shear stiffness is 0.10 from elastic stiffness.

Table (6): First and second critical flow velocity wit and without gyroscopic and soil damping (soft clay) at different pipe depth

Second mode with damping and gyroscopic	Second mode without damping and gyroscopic	First mode with damping and gyroscopic	First mode without damping and gyroscopic	Pipe depth (m)
15.261	15.394	14.854	14.867	0.5
16.733	16.901	16.721	16.746	1
18.826	19.089	18.811	18.826	2
Coupled mode flutter	buckling	buckling	Buckling	Instability type

As expected and shown in the table (5), the damping and gyroscopic effect have no an essential effect on the critical flow velocity on the first mode. However, they changes the type of instability of the second mode from buckling to coupled mode flutter.

Effect of internal pressure: Most of buried pipes are subjected to internal pressure of the carried fluid. Therefore, the effect of the internal pressure on the stability of such pipe is a point of interest. This effect on the critical flow velocity is investigated and shown in the figure (7). The first and second critical flow velocity at different pressure is calculated at pipe depth=1 m in soft clay soil.

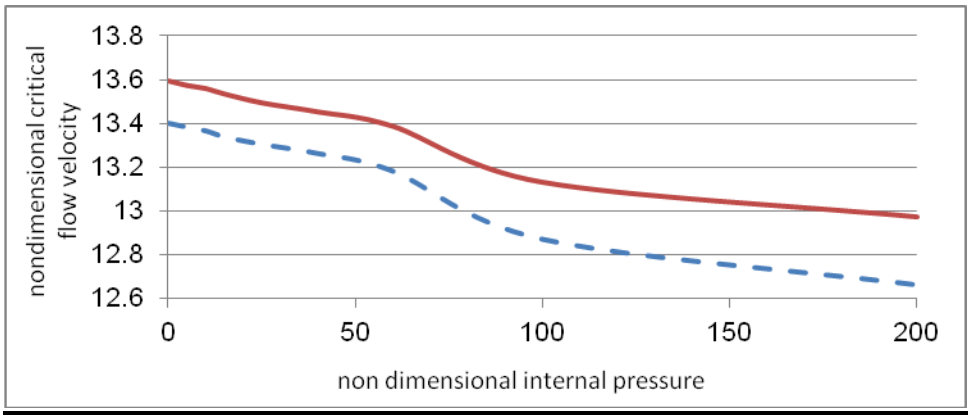

Figure (7): Change of critical flow velocities $V = vL_P\sqrt{\rho_f A_f / E\,\mathrm{I}}$ **with non-dimension pressure** $P = p \times L_p^2 A_p / (EI)$

From the above result, the internal pressure has an essential effect on the critical flow velocity especially in the range of (50-100). Numerically, at P=200, the internal pressure inside a pipe with outer diameter=0.12m and thickness= 1.5 cm is 288 MPa.

Conclusions:

An efficient mathematical model and a computer program for investigation of the dynamic and stability behavior of composite material pipes transporting a fluid and buried in soil have been implemented.

Composite material pipe transporting high flow velocity fluid has many design parameters can optimize the design to adapt the working condition. Soil type, fluid velocity, fluid pressure and pipe depth has a great effect on the behavior of such system. Damping and gyroscopic has no effect on the critical flow velocity, however, it has an effect on the instability type.

References:

[1] M.M. Maddah, S.H. Farghaly and E.M. Rabeih, 1992, Journal of engineering and applied science. “On the dynamic and stability behavior of a piping system conveying fluid.”, Vol. 39(3): June, pp: 551-566.

[2] M.M. Maddah, R.M.Gadelrab, E.M. Rabeih and A.A. Atwa, 2003, Engineering research journal, university of Helwan, “Dynamic behavior of composite pipes conveying steady fluid.”, Vol. 88, pp: M34-M48.

[3] E. Rabeih, M. El-Maddah, R. Gadelrab and A. Atwa, 2005, International journal of acoustics and vibration, “Effect of composite material parameters on vibrational behavior of pipes conveying fluid.”, Vol.10(2), pp: 93-97.

[4] L.C.Bank and C.-H.Kao, June 1990, Journal of energy resources technology “Dynamic response of thin walled composite material Timoshenko beams.”, Vol. 112, pp: 149-154.

[5] Jean H. Prevost and Radu Popescu, 1996, Journal of geotechnical engineering, ”Constitutive Relations for Soil Materials”, Vol.1.

[6] R.A. Jafari and M.T. Ahmadian, 2007, Journal of computer science, “Free vibration analysis of a cross ply laminated composite beam on Pasternak foundation.”, Vol. (3), pp: 51-57.

[7] Peijun Guo, Feb. 2005, Journal of geotechnical and geoenvironmental engineering, “Numerical modeling of pipe–soil interaction under oblique loading.", pp: 260-268.

[8] Park and M. A. Hashash, 2004, Journal of earthquake engineering, "Soil damping formulation in nonlinear time domain site response analysis.", Vol. 8(2), pp: 249-274.

[9] K.K Teoh and C. C. Huang, 1979, Journal of sound and vibration, “The vibration of generally orthotropic beams, a finite element approach.” Vol. 62, pp: 195-206.

[10] D. S. and M. Jr., H., 1973, Journal of composite materials, “Shear coefficient for orthotropic beam.”, Vol. 7, pp: 335-535.

[11] M.M. Maddah, R.M.Gadelrab, E.M. Rabeih and A.A.Atwa, 2003, Engineering research journal, university of Helwan, “Dynamic behavior of composite pipes conveying steady fluid.”, Vol. 88, pp: M34-M48.

[12] K.K Tea&C.C.Huang (1979) “Vibration of generally orthotropic beams”, Journal of sound and vibration, Vol. 62(2), pp 195-206.

[13] Parametric evaluation of seismic behavior of freestanding spent fuel dry cask storage systems, NUREG/CR-6865.
[14] M.M. Maddah, S.H. Farghaly and E.M. Rabeih, (1992), "On the dynamic and stability behavior of a piping system conveying fluid", Journal of engineering and applied science, Vol. 39, No 3 June, pp 551-566.
[15] R.A. Jafari and M.T. Ahmadian, 2007, Journal of computer science, "Free vibration analysis of a cross ply laminated composite beam on Pasternak foundation.", Vol. (3), pp: 51-57.
[16] Manjriker Gunaratne, 2006, Taylor and Francis Group. "Foundation engineering handbook".

Appendix A

Shape function elements for modified mass matrix

$$a_{25} = \left(-\left(2-12s^2\right)\zeta + 3\zeta^2\right)/(1+12s^2)$$
$$a_{26} = 0$$
$$a_{31} = \left(\left(6\alpha/\lambda\right)\xi - \left(6\alpha/\lambda\right)\xi^2\right)/(1+12s^2)$$
$$a_{32} = \left(\left(3\alpha/\lambda\right)\zeta - \left(3\alpha/\lambda\right)\zeta^2\right)/(1+12s^2)$$
$$a_{33} = 1-\zeta$$
$$a_{34} = \left(-\left(6\alpha/\lambda\right)\xi + \left(6\alpha/\lambda\right)\xi^2\right)/(1+12s^2)$$
$$a_{35} = \left(\left(3\alpha/\lambda\right)\zeta - \left(3\alpha/\lambda\right)\zeta^2\right)/(1+12s^2)$$
$$a_{36} = \zeta$$

$$a_{11} = \left(1+12s^2-12s^2\zeta-3\zeta^2+2\zeta^3\right)/(1+12s^2)$$
$$a_{12} = \left(\left(1+6s^2\right)\zeta - \left(2+6s^2\right)\zeta^2+\zeta^3\right)/(1+12s^2)$$
$$a_{13} = 0$$
$$a_{14} = (12s^2\zeta+3\zeta^2-2\zeta^3)/(1+12s^2)$$
$$a_{15} = \left(-6s^2\zeta - \left(1-6s^2\right)\zeta^2+\zeta^3\right)/(1+12s^2)$$
$$a_{16} = 0$$
$$a_{21} = \left(-6\zeta+6\zeta^2\right)/(1+12s^2)$$
$$a_{22} = \left(1+12s^2-\left(4+12s^2\right)\zeta+3\zeta^2\right)/(1+12s^2)$$
$$a_{23} = 0$$
$$a_{24} = \left(6\zeta-6\zeta^2\right)/(1+12s^2)$$

Appendix B

Shape function elements for modified stiffness matrix

$$b_{11} = \left(-12s^2-6\xi+6\xi^2\right)/\left(1+12s^2\right)$$
$$b_{12} = \left(1+6s^2-4\xi-12s^2\xi+3\xi^2\right)/\left(1+12s^2\right)$$
$$b_{13} = 0$$
$$b_{14} = \left(12s^2+6\xi-6\xi^2\right)/\left(1+12s^2\right)$$
$$b_{15} = \left(-6s^2-2\xi+12s^2\xi+3\xi^2\right)/\left(1+12s^2\right)$$
$$b_{16} = 0$$
$$b_{21} = \left(-6+12\xi\right)/\left(1+12s^2\right)$$
$$b_{22} = \left(-4=12s^2+6\xi\right)/\left(1+12s^2\right)$$
$$b_{23} = 0$$
$$b_{24} = \left(6-12\xi\right)/\left(1+12s^2\right)$$
$$b_{25} = \left(-2+12s^2+6\xi\right)/\left(1+12s^2\right)$$
$$b_{26} = 0$$

$$b_{31} = \left(6\frac{\alpha}{\lambda}-12\frac{\alpha}{\lambda}\xi\right)/\left(1+12s^2\right)$$
$$b_{32} = \left(3\frac{\alpha}{\lambda}-6\frac{\alpha}{\lambda}\xi\right)/\left(1+12s^2\right)$$
$$b_{33} = -1$$
$$b_{34} = \left(-6\frac{\alpha}{\lambda}+12\frac{\alpha}{\lambda}\xi\right)/\left(1+12s^2\right)$$
$$b_{35} = \left(3\frac{\alpha}{\lambda}-6\frac{\alpha}{\lambda}\xi\right)/\left(1+12s^2\right)$$
$$b_{36} = 1$$
$$b_{41} = \left(-6\xi+6\xi^2\right)/\left(1+12s^2\right)$$
$$b_{42} = \left(1+12s^2-4\xi-12s^2\xi+3\xi^2\right)/\left(1+12s^2\right)$$
$$b_{43} = 0$$

$$b_{44} = \left(6\xi-6\xi^2\right)/\left(1+12s^2\right)$$
$$b_{45} = \left(-2+12s^2\xi+3\xi^2\right)/\left(1+12s^2\right)$$
$$b_{46} = 0$$